Article

Cell Reports

Trapping of Syntaxin1a in Presynaptic Nanoclusters by a Clinically Relevant General Anesthetic

Graphical Abstract

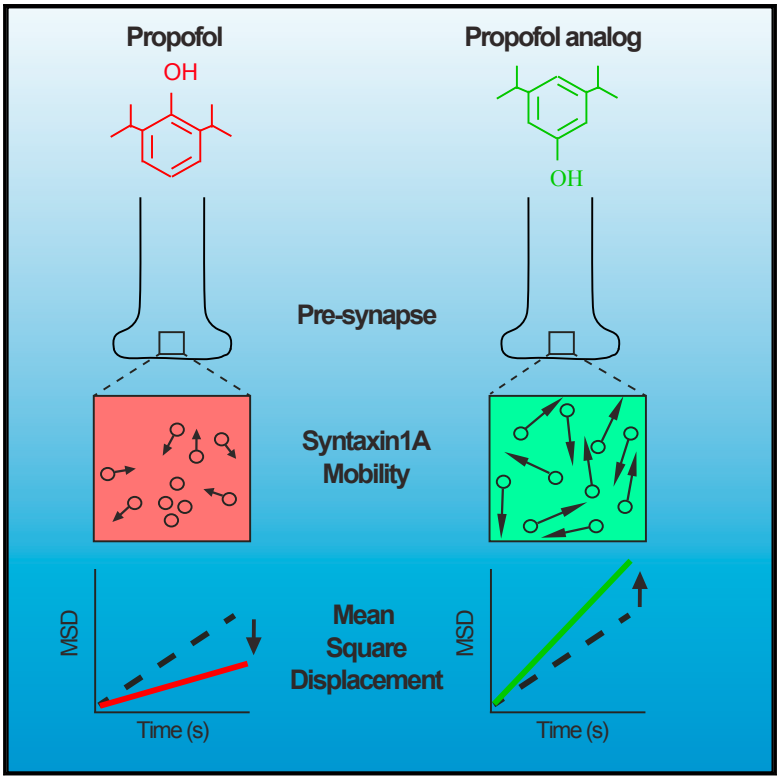

Authors

Adekunle T. Bademosi, James Steeves, Shanker Karunanithi, ..., Victor Anggono, Frederic A. Meunier, Bruno van Swinderen

Correspondence

b.vanswinderen@uq.edu.au

In Brief

Bademosi et al. use single-molecule imaging microscopy to understand how general anesthetics might affect presynaptic release mechanisms. They find that a clinically relevant concentration of propofol targets the presynaptic release machinery by specifically restricting syntaxin1A mobility on the plasma membrane. This suggests an alternate target process for these drugs.

Highlights

- Propofol impairs presynaptic release of neurotransmitters
- Propofol and etomidate restrict syntaxin1A mobility on presynaptic membranes
- Non-anesthetic analogs of propofol increase syntaxin1A mobility
- A propofol target emerges from an interaction between syntaxin1A and SNAP-25

Bademosi et al., 2018, Cell Reports *22*, 427–440
January 9, 2018
https://doi.org/10.1016/j.celrep.2017.12.054

CellPress

Cell Reports
Article

Trapping of Syntaxin1a in Presynaptic Nanoclusters by a Clinically Relevant General Anesthetic

Adekunle T. Bademosi,[1,2] James Steeves,[1] Shanker Karunanithi,[1,3] Oressia H. Zalucki,[1] Rachel S. Gormal,[1,2] Shu Liu,[1,2] Elsa Lauwers,[4] Patrik Verstreken,[4] Victor Anggono,[1,2] Frederic A. Meunier,[1,2] and Bruno van Swinderen[1,5,*]

[1]Queensland Brain Institute, The University of Queensland, Brisbane QLD 4072, Australia
[2]Clem Jones Centre for Ageing Dementia Research, Queensland Brain Institute, The University of Queensland, Brisbane QLD 4072, Australia
[3]School of Medical Science and Menzies Health Institute Queensland, Griffith University Gold Coast Campus, Gold Coast QLD 4222, Australia
[4]VIB Center for Brain and Disease Research, KU Leuven Department of Neurosciences, Leuven Institute for Neuroscience and Disease (LIND), 3000 Leuven, Belgium
[5]Lead Contact
*Correspondence: b.vanswinderen@uq.edu.au
https://doi.org/10.1016/j.celrep.2017.12.054

SUMMARY

Propofol is the most commonly used general anesthetic in humans. Our understanding of its mechanism of action has focused on its capacity to potentiate inhibitory systems in the brain. However, it is unknown whether other neural mechanisms are involved in general anesthesia. Here, we demonstrate that the synaptic release machinery is also a target. Using single-particle tracking photoactivation localization microscopy, we show that clinically relevant concentrations of propofol and etomidate restrict syntaxin1A mobility on the plasma membrane, whereas non-anesthetic analogs produce the opposite effect and increase syntaxin1A mobility. Removing the interaction with the t-SNARE partner SNAP-25 abolishes propofol-induced syntaxin1A confinement, indicating that syntaxin1A and SNAP-25 together form an emergent drug target. Impaired syntaxin1A mobility and exocytosis under propofol are both rescued by co-expressing a truncated syntaxin1A construct that interacts with SNAP-25. Our results suggest that propofol interferes with a step in SNARE complex formation, resulting in non-functional syntaxin1A nanoclusters.

INTRODUCTION

General anesthetics abolish consciousness and produce a behaviorally inert state that is conducive to surgery. Sedation induced by drugs such as propofol and etomidate is now understood to involve potentiation of GABA(A) receptors in sleep/wake circuits in the mammalian brain (Brown et al., 2011; Franks, 2008), but it remains unclear what other mechanisms might be responsible for the complete loss of behavioral responsiveness seen in all animals exposed to ''surgical'' concentrations of these drugs. Whereas general anesthetics target a variety of cellular functions over a wide range of drug concentrations (Franks, 2006; Franks and Lieb, 1994), there is growing evidence that clinically relevant doses of volatile anesthetics (e.g., isoflurane) as well as intravenous anesthetics (e.g., propofol and etomidate) also impair SNARE-mediated presynaptic neurotransmitter release mechanisms (Baumgart et al., 2015; Herring et al., 2009, 2011; Nagele et al., 2005; van Swinderen and Kottler, 2014; Xie et al., 2013). Genetic mutations in syntaxin1A, a key membrane-bound SNARE protein required for exocytosis (Südhof and Rizo, 2011; Südhof and Rothman, 2009), have also been shown to confer resistance to some general anesthetics *in vitro* (Herring et al., 2011; Herring et al., 2009) and *in vivo* (Zalucki et al., 2015), suggesting the neurotransmitter release machinery could also be targeted by these drugs. Recent investigations using single-molecule imaging have revealed that changes in synaptic activity are associated with altered syntaxin1A mobility on the plasma membrane of live neurosecretory cells and motor nerve terminals (Bademosi et al., 2017; Gandasi and Barg, 2014; Kasula et al., 2016). Here, we used single-particle tracking photoactivated localization microscopy (sptPALM) to track the mobility of individual syntaxin1A molecules in the presence of clinical doses of propofol and etomidate, the two most common intravenous anesthetics used for performing surgery in human patients.

RESULTS

Propofol Impairs Neurotransmission

In our first line of experiments, we confirmed that a clinically relevant concentration of propofol (3 μM; Sall et al., 2012) indeed impairs neurotransmitter release in three different live neural preparations: neurosecretory PC12 cells, cultured rat cortical neurons, and *Drosophila* larval motor neurons (Figure 1). Exposing PC12 cells to propofol (Figure 1A) significantly decreased evoked release of neuropeptide Y (NPY) (Figure 1B). We then expressed a genetically encoded reporter of neurotransmitter release, synaptophysin-pHluorin (sypHy) (Miesenböck et al., 1998), in rat cortical neuron cultures and measured exocytosis via unquenching of sypHy at synaptic boutons following neuronal activation (Figure 1C). Depolarization of neurons produced widespread synaptic release across the cultured neurons, an effect that was significantly compromised by 3 μM propofol (Figure 1D). A similar inhibitory effect of propofol on

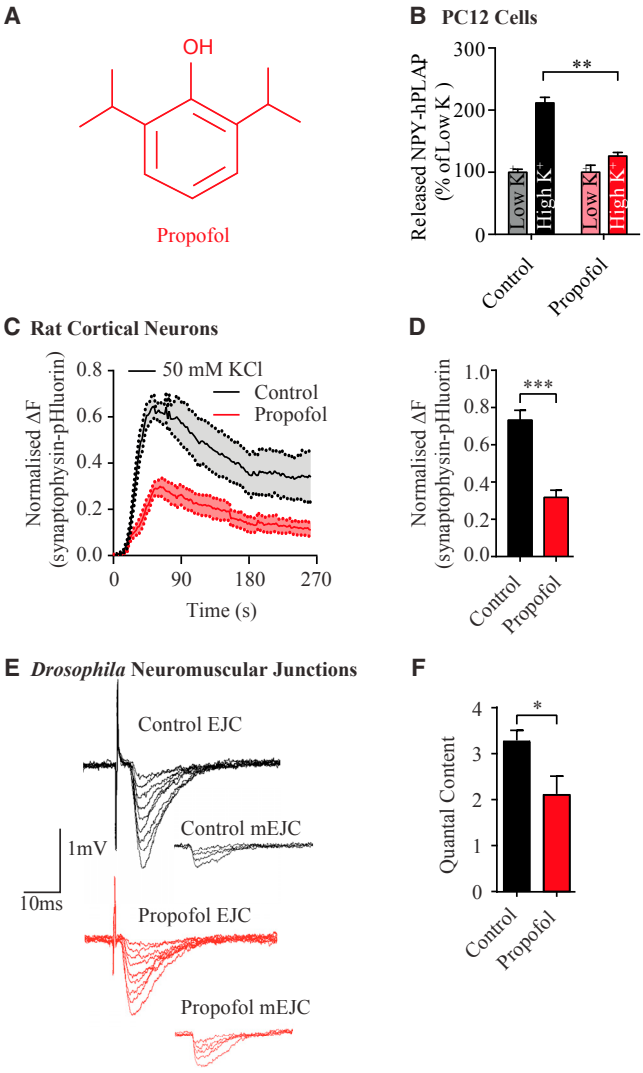

Figure 1. Propofol Decreases Neurotransmitter Release

The effect of propofol on neurotransmitter release was assayed *in vitro* and *in vivo*.

(A and B) Neurosecretory PC12 cells were transfected with NPY-hPLAP and pretreated for 5 min with either 3 μM of propofol (A) dissolved in DMSO or an equivalent amount of DMSO to control cells. Cells were treated with either low-K^+ or high-K^+ buffers to elicit secretion for 3 min (n = 3 control, n = 3 propofol). (B) The released NPY-hPLAP was measured by luminescence (Experimental Procedures) and expressed as a percentage of low-K^+ release. 3 μM propofol exposure significantly decreased NPY-hPLAP release.

(C) Rat cortical neurons were transfected with synaptophysin-pHluorin in order to visualize KCl-evoked synaptic release events. The curves show average synaptic intensity traces from neurons perfused with either buffer (control) or 3 μM propofol solution, normalized against the total releasable pool (Experimental Procedures).

(D) Propofol perfusion significantly decreased neurotransmitter release. Number of independent experiments (n) = 6 control, n = 5 propofol; >100 boutons per condition.

(E and F) At the *Drosophila* larval NMJ, a focal macropatch electrode was used to record spontaneous and evoked currents (E) generated by an individual type 1b synaptic bouton. Quantal content (F) was calculated from the ratio of evoked excitatory junctional currents (EJCs) to miniature excitatory junctional currents (mEJCs) (Experimental Procedures). Average EJC amplitude for controls, 0.51 ± 0.03; for propofol, 0.39 ± 0.05. Average mEJC amplitude for controls, 0.16 ± 0.01; for propofol, 0.20 ± 0.01 (n = 12 control, n = 12 propofol). All results are expressed as mean ± SEM. *p < 0.05, **p < 0.01, and ***p < 0.001 (unpaired Student's t test). See also Figure S1.

neurotransmitter release was detected with electrical stimulation of the neurons (Figures S1A and S1B). This is consistent with recent findings for volatile anesthetics in primary hippocampal neurons (Baumgart et al., 2015). To examine whether this effect was also evident at naturally formed glutamatergic synapses *in vivo*, we performed focal macropatch recordings (Karunanithi et al., 1999; Karunanithi et al., 2002) from individual boutons at the neuromuscular junction (NMJ) of larval *Drosophila melanogaster* flies (Figure 1E). We found that 3 μM propofol significantly decreased quantal release from individual boutons (Figures 1F and S1C–S1E), without affecting the frequency of non-evoked release events (mEJCs; Figure S1F). This is consistent with recent findings for isoflurane in a similar fly larval preparation (Zalucki et al., 2015). Together, these experiments across diverse systems indicate that a clinically relevant concentration of propofol potently disrupts neurotransmitter release and that this is a presynaptic effect. Importantly, the postsynaptic inhibitory ion channels that form the canonical target mechanism of propofol (Bali and Akabas, 2004; Franks, 2008) are unlikely to be involved in these presynaptic preparations. Other target mechanisms must therefore be present to significantly impair neurotransmission.

Propofol Restricts Syntaxin1A Mobility on the Cell Membrane

Like all general anesthetics, propofol is lipophilic and therefore inserts in the lipid bilayer of neurons (Franks, 2008; Tsuchiya, 2001). Key presynaptic release machinery proteins, such as syntaxin1A and SNAP-25, are organized in nanoclusters on the plasma membrane and can dynamically recruit vesicle-associated membrane protein 2 (VAMP2), leading to exocytosis at synaptic release sites (Sudhof, 2004; Südhof and Rizo, 2011). We hypothesized that, by segregating within the plasma membrane, propofol might compromise the function of membrane-bound SNARE proteins such as syntaxin1A. In order to assess the behavior of individual syntaxin1A proteins on the cell membrane, we tagged syntaxin1A with photoconvertible mEos2 (Figure 2A) and expressed this construct in PC12 cells (Figure 2Bi). mEos2 photoconversion allows single-molecule imaging in live cells by total internal reflection fluorescence (TIRF) microscopy (McKinney et al., 2009). Analysis of single particles of mEos2-tagged syntaxin1A (Figure 2Bii) allows quantification of diffusion coefficients of syntaxin1A on the plasma membrane (Figure 2Biii), as well as defining a super-resolved intensity map (Figure 2Bii). To quantify syntaxin1A dynamics (Movie S1), data from multiple trajectories (>3,000 trajectories per cell, 15–30 cells; Figure 2Ci) were combined to calculate the syntaxin1A-mEos2 mean square displacement (MSD) and diffusion coefficient frequency distribution (Figures 2D and 2E) in the presence or absence of propofol. As previously described (Barg et al., 2010; Gandasi and Barg, 2014), we detected a mobile and immobile population of syntaxin1A (Figures 2Cii and 2Ciii) indicative of syntaxin1A confinement

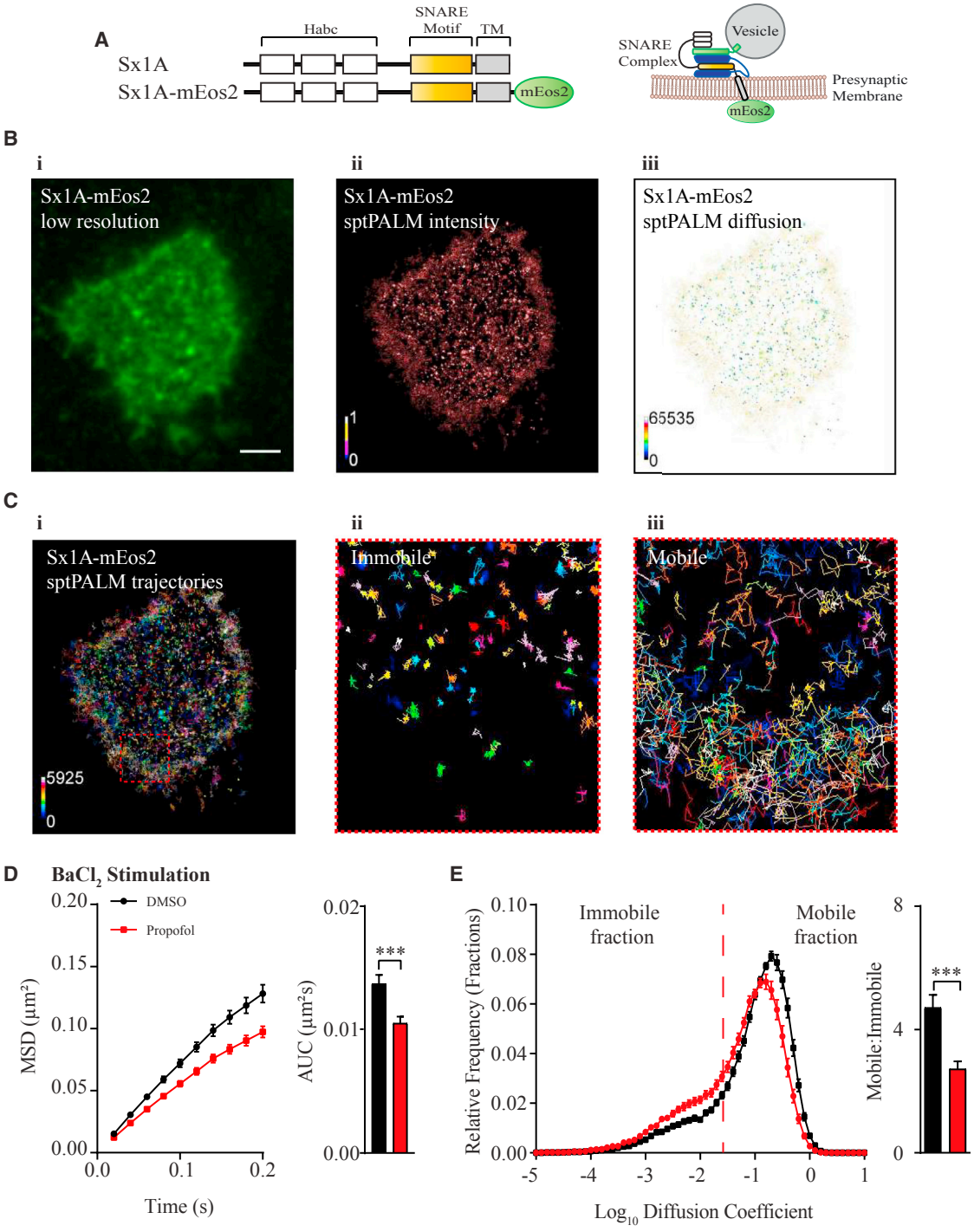

Figure 2. Propofol Decreases Syntaxin1A Mobility

(A) To carry out single-molecule tracking, syntaxin1A was tagged with a photoconvertible fluorescent protein, mEos2 on the C terminus of the molecule, adjacent to its transmembrane (TM) domain (left). The extracellular placement of mEos2 allows tracking of syntaxin1A dynamics on the plasma membrane (right).

(B) (i) Low-resolution TIRF image of PC12 cells transfected with syntaxin1A-mEos2 (Sx1A-mEos2). Scale bar, 3μm. Analysis of movies (Movie S1) generated (sptPALM) intensity (ii) and diffusion maps (iii).

(C) Trajectory (i) maps, color coded in arbitrary units (4,278 trajectories) were also generated. Analysis of syntaxin1A-mEos2 mobility revealed mobile and immobile populations (ii and iii).

(D) Mean square displacement (MSD) as a function of time for syntaxin1A-mEos2 in control-DMSO and 3 μM-propofol-perfused PC12 cells. Cells were stimulated with 2 mM $BaCl_2$.

(legend continued on next page)

within nanoclusters. The presence of 3 μM propofol within a preparation of stimulated PC12 cells (Heldman et al., 1989; Kasula et al., 2016) significantly decreased the displacement of membrane-bound syntaxin1A compared to DMSO controls (Figure 2D; summed area under the MSD curve [AUC] statistics shown to the right). DMSO alone had no effect on syntaxin1A mobility (Figures S2A and S2B). The immobilization effect of propofol was confirmed by plotting the diffusion coefficient distribution of syntaxin1A molecules, revealing an increased immobile fraction and a simultaneous decrease in the mobile fraction (Figure 2E; change in the mobile/immobile ratio shown to the right). We saw the same confining effects in unstimulated PC12 cells (Figures S2C and S2D), indicating that syntaxin1A mobility is impaired whether or not cells are stimulated. A clinically relevant concentration of another intravenous general anesthetic, etomidate (Franks, 2006; Giese and Stanley, 1983; Herring et al., 2011), decreased syntaxin1A mobility in the same way (Figures S3A–S3E). To confirm that the effect of propofol on syntaxin1A mobility is also relevant at synapses *in vivo*, we expressed a *Drosophila* mEos2-tagged syntaxin1A in flies and tracked the dynamics of the protein in larval NMJ boutons following genetic activation of motor neurons (Movie S2) (Bademosi et al., 2017). Exposure to 3 μM propofol significantly decreased syntaxin1A mobility at the fly NMJ in a similar way (Figures 3A–3C).

Propofol Traps Syntaxin1A before SNARE Complex Formation

We next investigated whether the mobility of a different SNARE protein, VAMP2, was also reduced by propofol. Vesicle-bound VAMP2, or synaptobrevin, interacts with membrane-bound syntaxin1A and SNAP-25 to form a fusion-ready ternary complex. Most of VAMP2 resides on synaptic vesicles inside the cell and is thus technically not accessible to our imaging of events on the plasma membrane. However, VAMP2 translocates to the plasma membrane following vesicle fusion events, where it remains bound to syntaxin1A and SNAP-25 prior to recycling (Sudhof, 2004; Südhof and Rizo, 2011). By tagging VAMP2 with mEos2 (Figure S4A) we were thus able determine whether VAMP2 mobility on the plasma membrane mirrored syntaxin1A in the presence of propofol, as this would indicate a post-SNARE time frame for the effect of propofol. Using our PC12 cell preparation (Figure S4B), we found that propofol had no effect on VAMP2-mEos2 mobility (Figure S4C–S4F), showing instead a tendency for increased mobility. Given that the three SNARE partners exist as a complex on the membrane only during or following vesicle fusion (Hayashi et al., 1994; Südhof and Rizo, 2011; Südhof and Rothman, 2009), our findings suggest that the effect of propofol on syntaxin1A mobility occurs prior to formation of the tetrameric complex. This result also shows that the immobilizing effect of propofol does not generalize to other molecules associated with the plasma membrane, pointing instead to a specific effect on pre-SNARE syntaxin1A.

Propofol Traps Syntaxin1A in Presynaptic Nanoclusters

Syntaxin1A is organized into nanodomains *in vitro* and *in vivo* (Bademosi et al., 2017; Sieber et al., 2007). As previous studies have suggested that syntaxin1A mobility within these nanodomains is confined (Bademosi et al., 2017; Bar-On et al., 2012; Gandasi and Barg, 2014), we next investigated whether the propofol-mediated decrease in syntaxin1A mobility was associated with corresponding changes in the size or density of syntaxin1A nanoclusters. To achieve this, we carried out single-molecule localization and cluster parameter measurements in fixed PC12 cells expressing syntaxin1A-mEos2 (Figure 4A, left; Experimental Procedures). Cluster maps of syntaxin1A-mEos2 were generated by calculating Ripley's K function (Figure 4A, middle), and the cluster parameters were plotted from the spatial distribution of the molecules using an autocorrelation function (Figure 4A, right) (Harper et al., 2016; Sengupta et al., 2013). Although the cluster radius remained unchanged under propofol in stimulated PC12 cells (Figure 4B), the density of syntaxin1A molecules increased significantly (by 3-fold) (Figure 4C), and the estimated number of molecules per cluster more than doubled (Figure 4D). Similar effects were observed in unstimulated cells (Figures 4E–4G), although in this case, the cluster radius also significantly increased (Figure 4E). The increase in the density of syntaxin1A molecules probably results from increased detection of syntaxin1A oligomers rather than any increased expression levels (Veatch et al., 2012). Although the number of molecules per cluster appears low (~10) compared to estimates from another study (Sieber et al., 2007), this may be an underestimate as the co-expressed syntaxin1A-mEos2 is probably mixed with endogenous syntaxin1A in the same clusters (Zilly et al., 2011). This suggests that syntaxin1A density may actually be greater than indicated by our detection methods. To confirm that the lateral trapping of syntaxin1A within nanoclusters due to propofol is also relevant at synapses *in vivo*, we performed the same analyses on fixed *Drosophila* NMJ tissue and found similar clustering effects (Figures 4H–4K). Interestingly, the estimated number of (tagged) syntaxin1A molecules per cluster is greater in *Drosophila* boutons than PC12 cells (~40 versus ~10, respectively), which may reflect the fact that these are active synapses. That propofol increased the density of syntaxin1A molecules in both suggests interference with a fundamental syntaxin1A process.

Non-anesthetic Propofol Analogs Increase Syntaxin1A Mobility on the Membrane

Propofol and etomidate have different molecular structures, yet both restrict syntaxin1A mobility on the cell membrane, arguing that this effect is linked to their common capacity to act as general anesthetics. To further investigate this, we tested the effect of two propofol analogs, 2,4-diisopropylphenol and 3,5-diisopropylphenol, which closely resemble propofol but are not general anesthetics (Krasowski et al., 2001). These compounds differ from

(E) The change in mobility was quantified statistically by calculating the area under the MSD curve (AUC). The diffusion coefficient distribution of syntaxin1A-mEos2 ranged from 10^{-5} to 10^{-1} $\mu m^2/s$. The ratio of the mobile to immobile populations significantly decreased upon propofol perfusion (n = 17–22 cells from 3 independent experiments).

Results are expressed as mean ± SEM. ***p < 0.001 (unpaired Student's t test). See also Figures S2–S4.

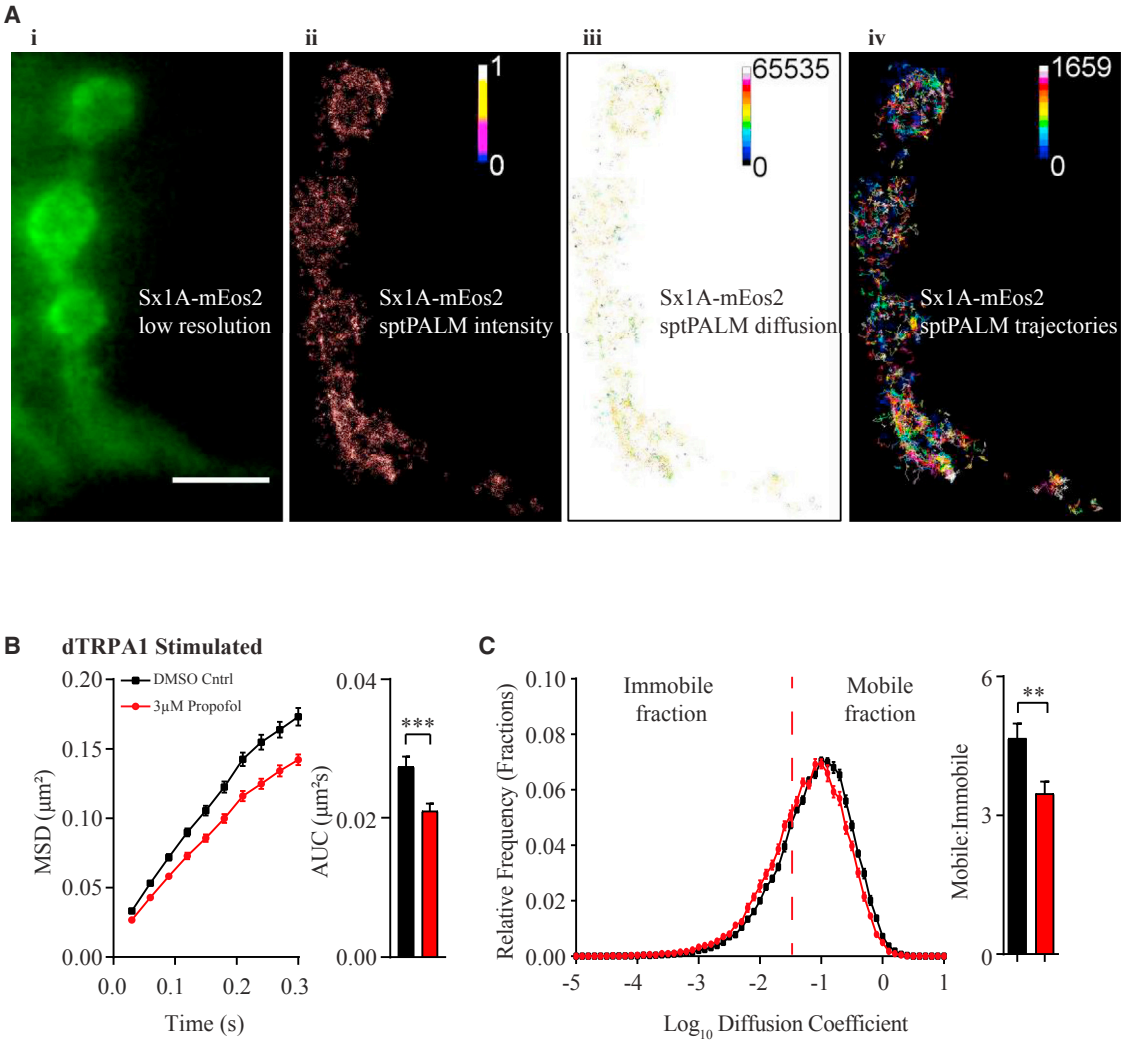

Figure 3. Propofol Decreases Syntaxin1A Mobility *In Vivo* in Activated *Drosophila* Larva Motor Nerve Terminals

(A) Slightly oblique illumination was used localize single-molecule mobility of syntaxin1A-mEos2 in transgenic *Drosophila melanogaster* third-instar larvae (Movie S2). Low-resolution TIRF image of a type 1b NMJ chain expressing syntaxin1A-mEos2 prior to photoconversion (i). SptPALM average intensity, diffusion coefficient, and trajectory of syntaxin1A-mEos2 (1,742 trajectories) (ii–iv). Scale bar, 5 μm.

(B) Mean square displacement (MSD) as a function of time of syntaxin1A-mEos2 in control (DMSO) and propofol-perfused *Drosophila* larvae expressing dTRPA1 at 30°C. Change in mobility was quantified statistically from the AUC.

(C) Diffusion coefficient distribution of syntaxin1A-mEos2. The ratio of the mobile to immobile populations significantly decreased upon propofol perfusion. n = 17–19 NMJ chains from 3 independent experiments.

Results are expressed as mean ± SEM. **p < 0.01 and ***p < 0.001 (unpaired Student's t test).

propofol by the position of a hydroxyl group on the benzene ring (Figure 5A). Apart from this, the analogs are identical to propofol in structure and molecular weight, and both are equally lipophilic (Krasowski et al., 2001; Tsuchiya, 2001). Interestingly, the analogs had the opposite effect to propofol on syntaxin1A mobility on the cell membrane; both significantly increased syntaxin1A mobility, in stimulated and unstimulated cells (Figures 5B–5E), consistent with their lipophilic property on membrane fluidity (Bahri et al., 2007; Tsuchiya, 2001; Tsuchiya et al., 2010). This suggests that the observed decrease in syntaxin1A mobility seen with propofol is linked to its anesthetic quality rather than its lipophilic nature. This also suggests that propofol specifically interacts with syntaxin1A or other SNARE partners. One of the key syntaxin1A partners immediately prior to SNARE formation is SNAP-25 (Nagele et al., 2005; Weiser et al., 2013). Therefore, we next assessed the role of this interaction in mediating the effect of propofol on syntaxin1A mobility.

Interaction with SNAP-25 Is Necessary for Propofol-Mediated Trapping

SNAP-25 has been shown to form dimers with syntaxin1A on the plasma membrane (Rickman et al., 2004), where both interact with VAMP2 and a number of accessory proteins such as Munc13 and Munc18 to form SNARE complexes (Weninger et al., 2008;

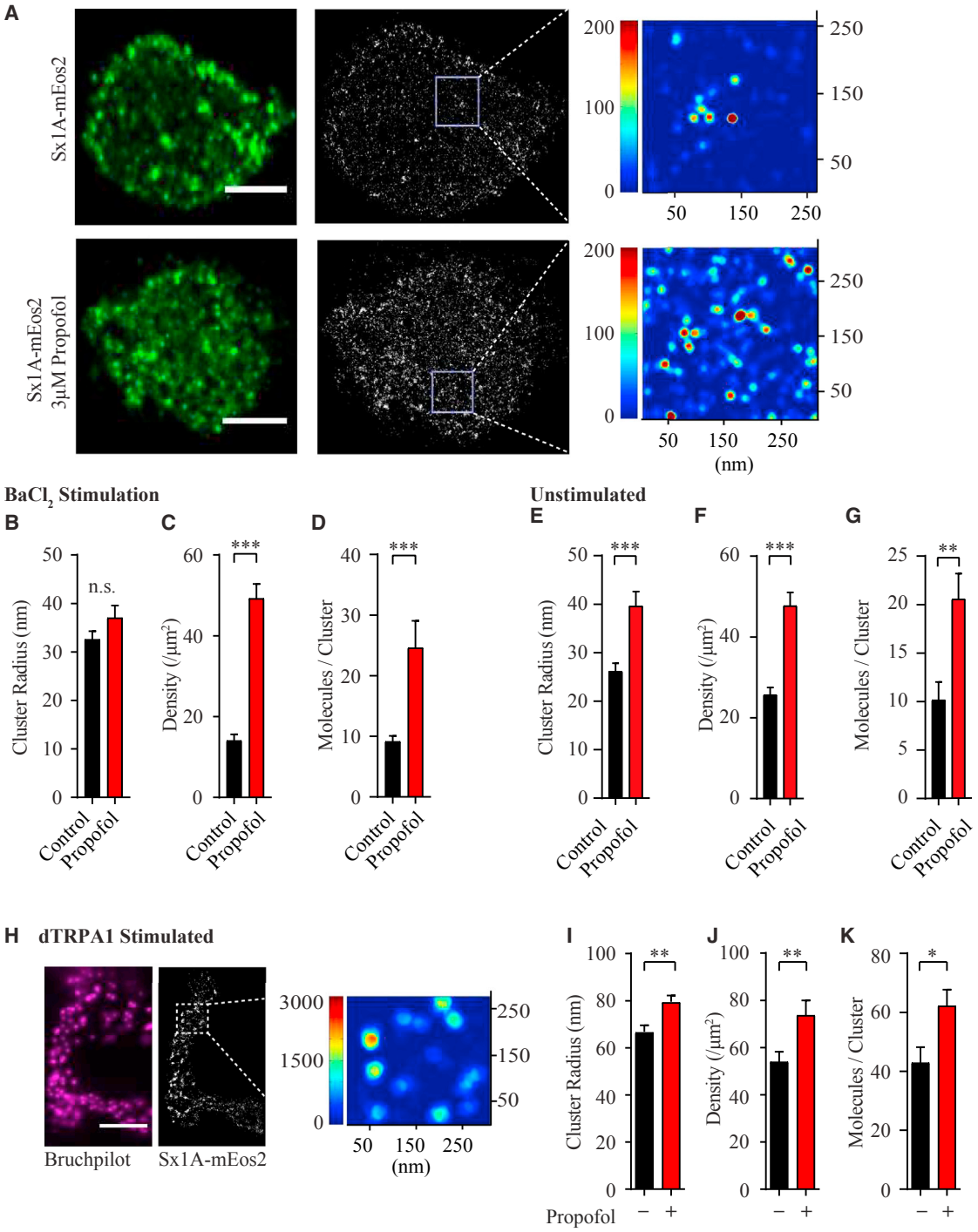

Figure 4. Propofol Traps Syntaxin1A in Nanoclusters *In Vitro* and *In Vivo*

Syntaxin1A-mEos2-transfected PC12 cells were fixed with paraformaldehyde before single-molecule localization (SML) imaging and processing.

(A) Left, representative low-resolution TIRF image; middle, the corresponding SML image; and right, the density map of the region of interest generated from Ripley's K-function of control-DMSO (top row) and 3 μM-propofol-perfused (bottom row) cells. Scale bar, 5 μm.

(B–D) The cluster radius (B), average density (C), and number of molecules per cluster (D) were obtained from each region of interest by fitting the autocorrelation values. Three regions of interest were analyzed per cell (n = 28–50 $BaCl_2$–stimulated cells from 3 independent experiments).

(E–G) Cluster radius (E), density (F), and molecules per cluster (G) of localization of syntaxin1A-mEos2 in unstimulated cells (n = 28–49 unstimulated cells from 3 independent experiments).

(legend continued on next page)

Xiao et al., 2001). If an interaction between SNAP-25 and syntaxin1A is required for propofol-mediated trapping of syntaxin1A in nanoclusters, then removing this interaction should eliminate the effect of propofol on syntaxin1A mobility. SNAP-25 interacts specifically with the SNARE motif of syntaxin1A (gold segment in Figure 6A, top) prior to forming a quadruple helix when both t-SNAREs meet with vesicle-bound VAMP2 (Weninger et al., 2008; Xiao et al., 2001). We reasoned that removing the SNARE motif from syntaxin1A might remove the propofol target and effectively abolish the effect of propofol on syntaxin1A mobility. To test this, we generated mEos2-tagged syntaxin1A deletion constructs in which the SNAP-25-interacting SNARE motif was entirely or partially removed (Figure 6A, middle and bottom). Removing all ($Sx1A^{\Delta 183–265}$) or part ($Sx1A^{\Delta 204–250}$) of the SNARE motif from syntaxin1A abolished the interaction with SNAP-25 (Figure 6B) as expected (Wu et al., 1999). Preventing this interaction with SNAP-25 or potentially also syntaxin1A homophilic interactions (Merklinger et al., 2017; Sieber et al., 2007) led to an increase in the mobility of $Sx1A^{\Delta 204–250}$-mEos2 compared to wild-type (Figure 6C, gray versus black; Figures S5A and S5B). Most importantly, the addition of propofol not only failed to restrict the mobility of $Sx1A^{\Delta 204–250}$-mEos2 but also increased mobility of the mutant protein even further (Figure 6C, brown; Figures S6A and S6B), regardless of stimulation (Figures 6D, S5C, and S5D). Repeating these experiments with the entire SNARE motif removed ($Sx1A^{\Delta 183–265}$-mEos2) revealed similar, but not identical, results (Figures S5E and S5F).

Recent studies have found an overlap between syntaxin1A and SNAP-25 clusters (Pertsinidis et al., 2013; Rickman et al., 2004), supporting the idea that these molecules could interact to form a joint propofol target. However, in the preceding experiments, we could not exclude the possibility that proteins other than SNAP-25 might be required for the propofol effect on syntaxin1A clustering, also because the SNARE motif of syntaxin1A has been shown to drive homophilic interactions of the protein (Sieber et al., 2007). To confirm that the effect of propofol on syntaxin1A mobility is indeed SNAP-25 dependent, we co-expressed syntaxin1A-mEos2 with botulinum neurotoxin E light chain (BoNT/E-LC), which cleaves SNAP-25 and therefore prevents formation of SNAP-25-syntaxin1A heterodimers on the plasma membrane (Hayashi et al., 1994; Rickman et al., 2004). BoNT/E-LC expression does not significantly alter syntaxin1A mobility (Figures S6A and S6B) as has also been shown previously (Kasula et al., 2016; Ribrault et al., 2011). However, it completely abolished propofol's immobilizing effect and instead led to increased syntaxin1A mobility (Figures 6E, 6F, S6C, and S6D). BoNT/E-LC also abolished the clustering effects seen under propofol (Figures 6G–6J and S6E–S6G). A simple model summarizing our results so far (Figure 6K) thus proposes that propofol-induced immobilization of syntaxin1A requires interaction with SNAP-25, most likely prior to SNARE complex assembly.

A Truncated Syntaxin1A Rescues Exocytosis and Mobility Effects of Propofol

We have shown that propofol impairs exocytosis (Figure 1) and propose that this is a consequence of syntaxin1A immobilization or clustering (Figures 2, 3, 4, 5, and 6). Although we have not yet established such causality, our model predicts that genetic manipulations affecting one presynaptic readout (syntaxin1A mobility) should also affect the other readout (exocytosis). Previous work has found that co-expression of a truncated isoform of syntaxin1A ($Sx1A^{227}$; Figure 7A) rescues the effect of propofol on exocytosis in PC12 cells (Herring et al., 2011). We therefore tested whether this genetic manipulation also rescued the effect of propofol on syntaxin1A mobility. We first confirmed that the construct indeed rescued evoked exocytosis (Figure 7B). We added a hemagglutinin (HA) tag at the N terminus of the truncated construct (Figure 7A, red) to determine whether it interacted with functional SNARE proteins, including wild-type syntaxin1A (tagged with mEos2), SNAP-25 (tagged with *Myc*), and VAMP2 (tagged with GFP). Co-immunoprecipitation experiments (Experimental Procedures) showed it interacts with SNAP-25, but not VAMP2 (Figures 7C and 7D). $Sx1A^{227}$ also interacts with wild-type syntaxin1A, alongside SNAP-25 (Figure 7E). This suggests a direct effect on functional syntaxin1A/SNAP-25 dimers rather than a parallel effect unrelated to SNARE formation.

We next co-transfected PC12 cells with wild-type syntaxin1A-mEos2 and $Sx1A^{227}$ (Figures S7A–S7C) and tracked syntaxin1A-mEos2 mobility in the presence and absence of propofol. Adding $Sx1A^{227}$ to the cells had no effect on syntaxin1A mobility in the absence of propofol (Figures S7D and S7E). However, adding the truncated construct abolished the effect of propofol on syntaxin1A mobility in both stimulated and unstimulated cells (Figures 7F, 7G, S7F, and S7G). This shows that the same manipulation in PC12 cells (co-expressing $Sx1A^{227}$) rescues both exocytosis and syntaxin1A mobility, suggesting that these presynaptic effects of propofol are linked.

DISCUSSION

This study demonstrates that clinical concentrations of a commonly used GABA-acting general anesthetic, propofol, also restrict syntaxin1A mobility on the plasma membrane. The contrast seen with the effect of propofol analogs is particularly striking, with the non-anesthetic analogs significantly increasing syntaxin1A mobility instead. Our results indicate that propofol acts like its non-anesthetic analogs when the interaction between syntaxin1A and SNAP-25 is lost, suggesting that propofol targets this interaction to immobilize syntaxin1A. It seems plausible that syntaxin1A confinement to nanoclusters could lead to impaired neurotransmission, which we also observe under propofol. However, more work is needed to establish causality

(H) Larvae expressing Sx1A-mEos2 and dTRPA1 were preheated at 30°C, dissected, paraformaldehyde-fixed, and processed for active zone immunostaining before single-molecule localization (SML) of Sx1A-mEos2. Representative low-resolution bruchpilot image of synaptic active zones (left), the corresponding SML image (middle), and the density map of the region of interest generated from Ripley's K-function (right). Scale bar, 5 μm.

(I–K) The cluster radius (I), average density (J), and number of molecules per cluster (K) of Sx1A-mEos2 were obtained from each region of interest by fitting the autocorrelation values (n = 31–32 NMJ chains from 3 independent experiments).

Results are expressed as mean ± SEM. *$p < 0.05$, **$p < 0.01$, and ***$p < 0.001$ (unpaired Student's t test).

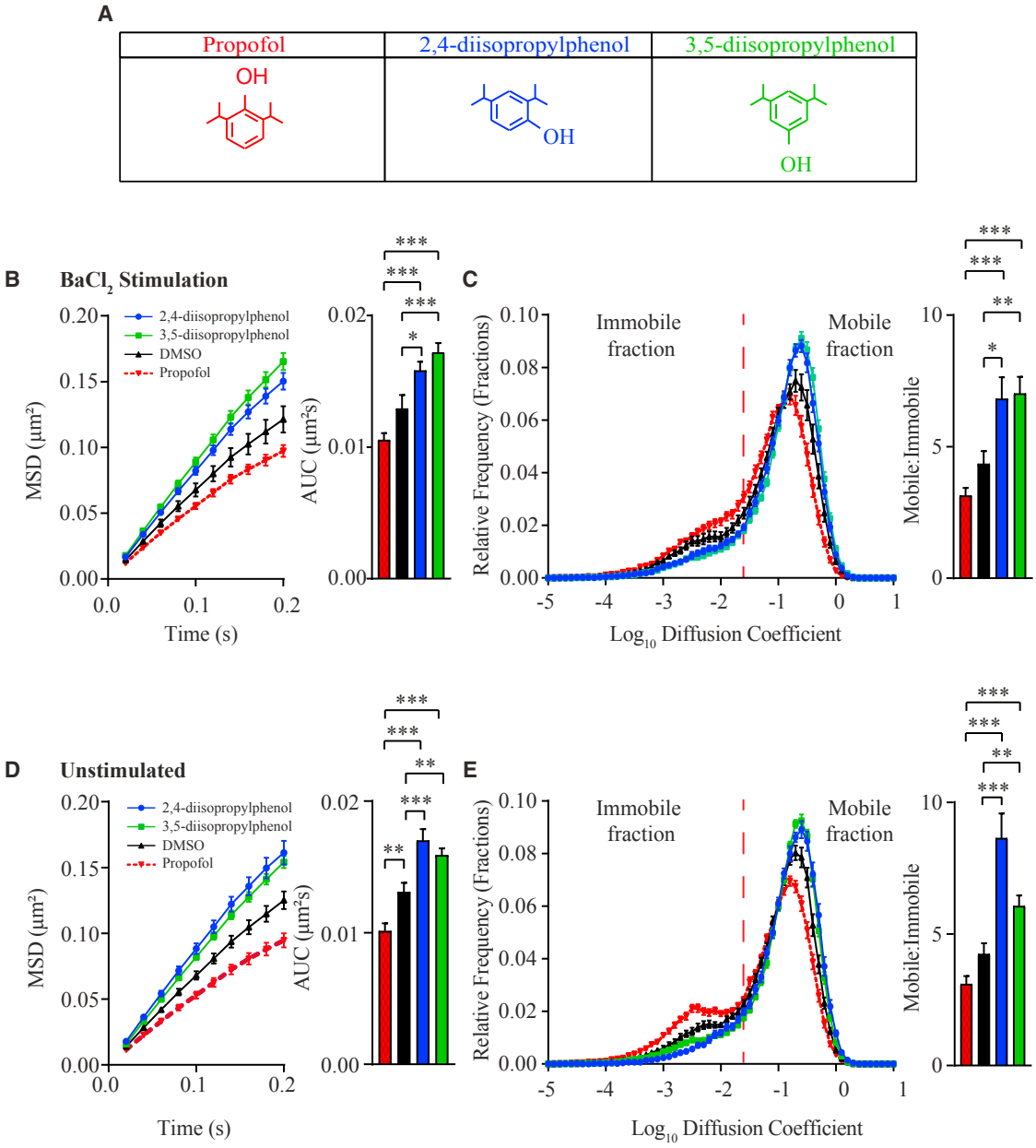

Figure 5. Propofol Analogs Increase Syntaxin1A Mobility

(A) Propofol structure compared to two non-anesthetic analogs, 2,4-diisopropylphenol (blue) and 3,5-diisopropylphenol (green).

(B) MSD of syntaxin1A-mEos2 in $BaCl_2$-stimulated PC12 cells perfused with 3 μM propofol, 3 μM 2,4-diisopropylphenol, or 3 μM 3,5-diisopropylphenol. The AUC reveals a significant increase in syntaxin1A-mEos2 mobility upon perfusion with the analogs.

(C) Diffusion coefficient distribution of syntaxin1A-mEos2 in cells exposed to propofol (red) and propofol analogs (blue and green) compared to control (black). Analysis of mobile to immobile ratios revealed a significant increase in syntaxin1A-mEos2 mobility when exposed to the analogs. For each condition, n = 17–21 cells from 3 independent experiments. Results are expressed as mean ± SEM.

(D) MSD of syntaxin1A-mEos2 in unstimulated PC12 cells perfused with 3 μM propofol and 3 μM non-anesthetic analogs. The AUC reveals a significant increase in syntaxin1A-mEos2 mobility upon perfusion with the analogs.

(E) Mobile to immobile ratios of the diffusion coefficient distributions also revealed a significant increase. For each condition, n = 18–30 cells from 3 independent experiments. Results are expressed as mean ± SEM. Comparisons were performed using one-way ANOVA with Tukey's multiple comparison test (*$p < 0.05$, **$p < 0.01$, and ***$p < 0.001$).

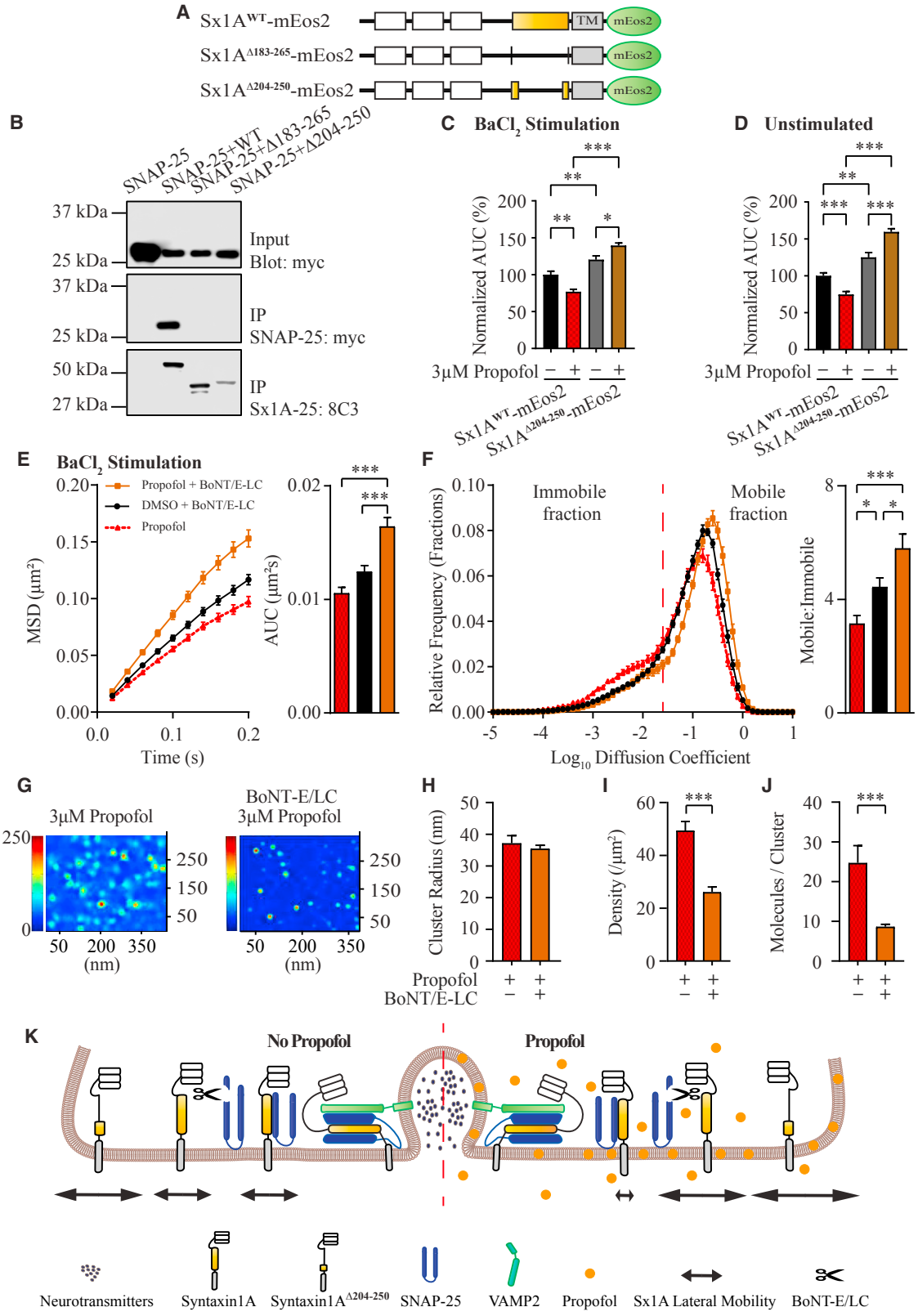

(legend on next page)

here. How exactly propofol impairs syntaxin1A mobility remains unclear, although the requirement for SNAP-25 interaction suggests the nanoclusters are composed of syntaxin1A/SNAP-25 heterodimers that have been blocked from proceeding to a subsequent step in SNARE complex formation due to the presence of the general anesthetic. It is also unclear how a truncated syntaxin1A protein might preserve this process against the effects of propofol on syntaxin1A mobility and exocytosis. Our finding that the truncated syntaxin1A molecule simultaneously interacts with both SNAP-25 and wild-type syntaxin1A suggests occupancy of a site that might otherwise be targeted by propofol. In this regard, future experiments with other truncation constructs (Metz et al., 2007) employing propofol resistance as a readout will be helpful toward determining whether the effects on syntaxin1A mobility and exocytosis are indeed correlated.

In addition to identifying an alternative target process for this widely used sedative, our findings may provide a more complete understanding of general anesthesia. Every neuron communicates with other neurons by way of syntaxin1A-mediated neurotransmission, which is highly conserved from worms to humans (Ferro-Novick and Jahn, 1994). Although our experiments were focused on the intravenous drugs propofol and etomidate, it will be interesting to see in future studies whether other general anesthetics have the same effect on syntaxin1A mobility. There is already considerable evidence that a broader range of general anesthetics affect synaptic release mechanisms (Herring et al., 2009, 2011; Xie et al., 2013), and a previous study using nuclear magnetic resonance found that clinical concentrations of these drugs interact with syntaxin1A and SNAP-25, but not VAMP2 (Nagele et al., 2005; Weiser et al., 2013), which is consistent with our conclusion that propofol acts before completed SNARE formation. One hypothesis consistent with our findings would be that a general anesthetic target emerges only when syntaxin1A and SNAP-25 interact on the plasma membrane and that the association of propofol with this emergent target interferes with subsequent steps in SNARE formation. This would lead to a "traffic jam" of syntaxin1A/SNAP-25 heterodimers (or another pre-SNARE moiety), which would manifest as syntaxin1A nanoclusters in our analysis. Another explanation for the decrease in syntaxin1A mobility could be that propofol promotes its recruitment into nonfunctional SNARE complexes that do not promote vesicle fusion (Bajohrs et al., 2004; Weninger et al., 2003). Whereas our data suggest interactions in the membrane, this need not be the only explanation for altered syntaxin1A mobility. An alternative possibility is that anesthetics might alter syntaxin1A mobility by more specifically interfering with other key protein interactions leading to SNARE formation, such as between syntaxin1A/SNAP-25 and Munc-13 (Metz et al., 2007), which is a crucial mediator in forming the final tetrameric complex with VAMP2 (Wang et al., 2017; Yang et al., 2015). Future experiments testing the effects of mutating candidate residues in the syntaxin1A SNARE motif should reveal the exact nature of this propofol-binding target, as has been revealed for other propofol targets, such as $GABA_A$ receptors (Yip et al., 2013) and TRPA1 channels (Ton et al., 2017).

Like sleep, general anesthesia resembles a reversible switch, and the search for mechanisms of anesthesia has justifiably focused on proteins that exert major effects on neuronal excitability, such as inhibitory $GABA_A$ receptors, which are indeed targets of many general anesthetics (Rudolph and Antkowiak, 2004). However, our results and the work of others show that clinically relevant concentrations of general anesthetics also compromise neurotransmitter release (Baumgart et al., 2015; Herring et al., 2009, 2011; Xie et al., 2013; Zalucki et al., 2015), and our current set of results with intravenous drugs suggests this may be consequence of effects on syntaxin1A mobility in the plasma membrane. However, general anesthetics do not abolish neurotransmission; they only decrease quantal content (Figure S1C). So how could this be relevant to the behavioral endpoint that is general anesthesia? With most animal brains comprising anywhere between millions and trillions of synapses, it seems plausible that normal brain functions would be compromised if syntaxin1A mobility became globally restricted across a variety of synapses following exposure to general anesthetics. While a decrease in quantal content may not significantly impair some muscular (or spinal cord) functions, it is likely that a similar effect on central synapses would dramatically change temporal dynamics in the brain, leading to a loss of functional connectivity. In support of this view, recent electroencephalogram (EEG) and fMRI studies have shown that functional

Figure 6. SNAP-25 Interaction Is Required for Propofol-Mediated Trapping of Syntaxin1A

(A) Schematic representation of the protein domains deleted from the syntaxin1A tagged with mEos2. Syntaxin1A$^{\Delta 183–265}$-mEos2 has residues deleted from 183–265, whereas syntaxin1A$^{\Delta 204–250}$-mEos2 was deleted from 204–250 (Table S1).

(B) Co-immunoprecipitation of SNAP-25 with syntaxin1A-mEos2 and deletion mutants. Loss of the SNARE motif prevents the interaction between syntaxin1A and SNAP-25.

(C and D) MSD AUC for syntaxin1A deletion mutants in $BaCl_2$-stimulated and unstimulated cells normalized against syntaxin1A-mEos2 in DMSO control cells. For each condition, n = 17–30 cells from 3 independent experiments. Comparisons were performed using one-way ANOVA with Tukey's multiple comparison test (*$p < 0.05$, **$p < 0.01$, and ***$p < 0.001$).

(E) MSD of syntaxin1A-mEos2 in stimulated PC12 cells transfected with BoNT-E/LC. The AUC showed significant increase in syntaxin1A-mEos2 mobility in cells perfused with propofol (3 μM) compared with DMSO control cells.

(F) Diffusion coefficient distribution of syntaxin1A-mEos2 in BoNT-E/LC expressing cells with and without propofol. Analysis of the mobile to immobile ratios revealed a significant increase in syntaxin1A-mEos2 in the presence of BoNT-E/LC and propofol. n = 15–23 cells from 3 independent experiments. Results are expressed as mean ± SEM. Comparisons were performed using one-way ANOVA with Holm-Sidak's multiple comparison test (*$p < 0.05$ and ***$p < 0.001$).

(G) Density map of syntaxin1A-mEos2 in 3 μM propofol-perfused cells with and without BoNT-E/LC.

(H–J) The cluster radius (H), average density (I), and number of molecules per cluster (J) of syntaxin1A-mEos2 in PC12 cells expressing BoNT-E/LC. For each condition, n = 32–50 cells from 3 independent experiments. Results are expressed as mean ± SEM. ***$p < 0.001$ (unpaired Student's t test). See also Figures S5 and S6.

(K) Model showing changes in syntaxin1A lateral mobility on the plasma membrane. Propofol restricts syntaxin1A mobility and this decrease is tightly coupled to interaction with SNAP-25, as shown by the cleavage of SNAP-25 with BoNT-E/LC or by deletion of syntaxin1A SNARE motif. See also Figures S5 and S6.

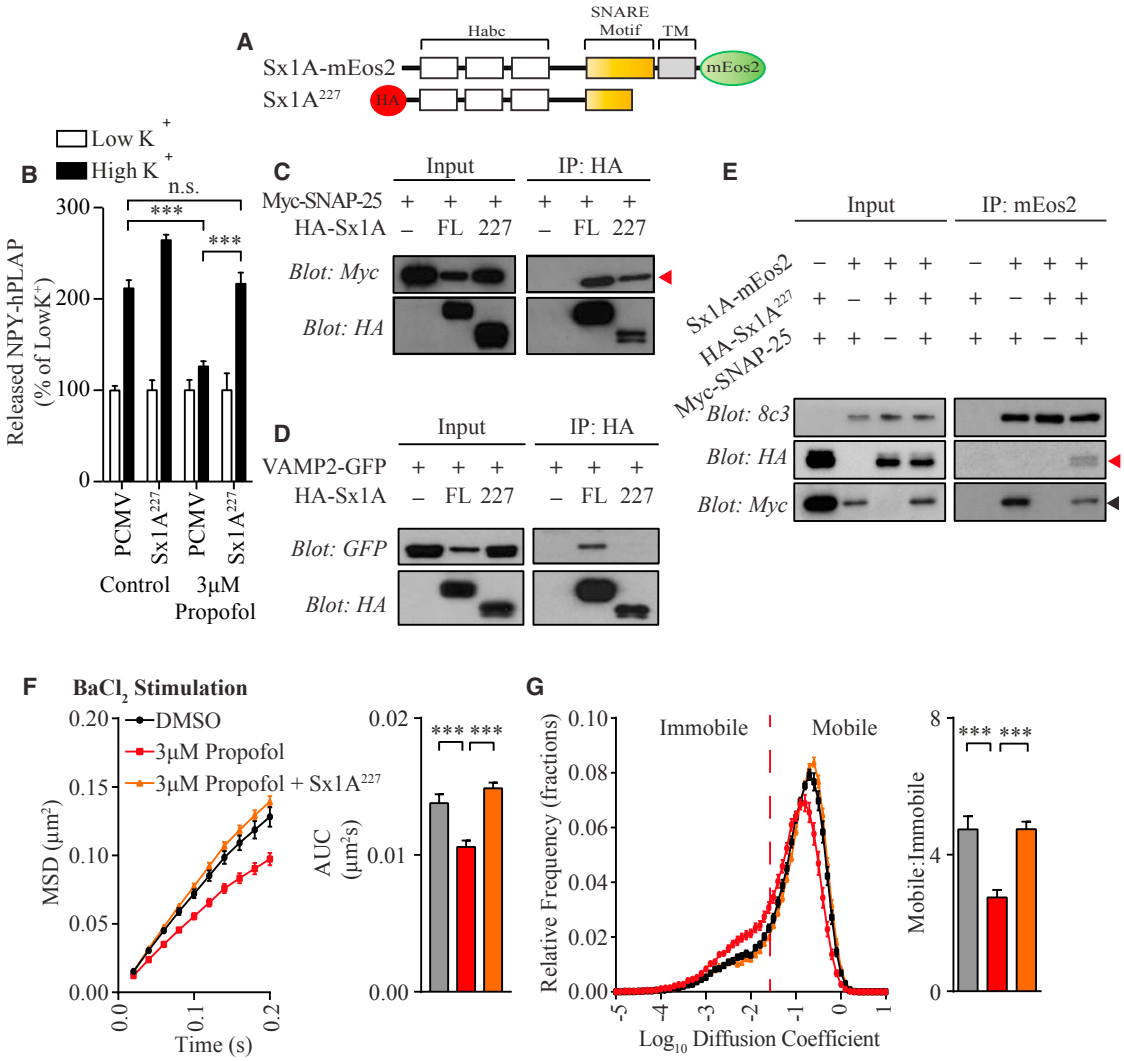

Figure 7. Decreased Neurotransmitter Release and Syntaxin1A Mobility Is Rescued by a Truncated Syntaxin1A Protein

(A) Schematic representation of syntaxin1A-mEos2 and the truncated syntaxin1A protein syntaxin1A^{227} tagged with an HA tag.

(B) NPY-hPLAP was co-transfected into PC12 cells with either an empty vector (PCMV) or syntaxin1A^{227}. Cells were pretreated for 5 min with either 3 μM of propofol or DMSO. Cells were treated with either low-K$^+$ or high-K$^+$ buffers to elicit secretion for 3 min (n = 3 control, n = 3 propofol). Propofol decreased NPY-hPLAP release in PCMV transfected cells, but not in syntaxin1A^{227} transfected cells. The released NPY-hPLAP was expressed as a percentage of low-K$^+$ release. 3 μM propofol exposure significantly decreased NPY-hPLAP release.

(C) Co-immunoprecipitation experiment testing for interaction between the HA-tagged truncated syntaxin1A and Myc-tagged SNAP-25. Red arrowhead points to successful pull-down of the truncated syntaxin1A protein with SNAP-25.

(D) Co-immunoprecipitation experiment testing interaction between the HA-tagged truncated syntaxin1A protein and GFP-tagged VAMP2.

(E) Co-immunoprecipitation experiment testing for interaction among mEos2-tagged full-length syntaxin1A, HA-tagged truncated syntaxin1A, and Myc-tagged SNAP-25. Red arrowhead points to successful pull-down of the truncated syntaxin1A protein by the full-length protein via a SNAP-25 interaction (black arrowhead). 8c3 is an antibody recognizing the wild-type syntaxin1A protein.

(F) MSD of syntaxin1A-mEos2 in $BaCl_2$-stimulated PC12 cells decreased upon propofol perfusion. In PC12 cells co-transfected with syntaxin1A^{227}, syntaxin1A-mEos2 mobility was unaffected by propofol. The AUC showed significant decrease in syntaxin1A-mEos2 mobility in cells perfused with propofol (3 μM, red) but no decrease in syntaxin1A^{227} transfected cells (orange).

(G) Diffusion coefficient distribution of syntaxin1A-mEos2 in syntaxin1A^{227}-expressing cells upon propofol perfusion. Same experiments as in (F). Analysis of the mobile to immobile ratios revealed a significant decrease in syntaxin1A-mEos2 in the presence propofol; this decrease was abolished in syntaxin1A^{227}-expressing cells. n = 19–32 cells from 3 independent experiments. Results are expressed as mean ± SEM. Comparisons were performed using one-way ANOVA with Tukey's multiple comparison test (***p < 0.001). See also Figure S7.

connectivity throughout the brain is significantly altered in patients undergoing general anesthesia (Boly et al., 2012; Chennu et al., 2016; Hudetz, 2012; Lewis et al., 2012). Thus, other manipulations that compromise presynaptic communication, including effects on presynaptic excitability (Baumgart et al., 2015), might fall into the same category of anesthetic mechanisms as the

syntaxin1A-mediated effects we describe here, which may be considered a class of effects that is distinct from GABAergic sleep-related mechanisms. One possibility, which we have raised previously (van Swinderen and Kottler, 2014), is that GABAergic processes (e.g., sedation and loss of consciousness) are induced at lower drug doses (e.g., <1 μM propofol; Franks and Lieb, 1994), while the presynaptic processes discussed here are affected at the slightly higher concentrations required for surgery. It remains unknown however whether other general anesthetics target presynaptic mechanisms. A recent study using hippocampal cultures found that isoflurane inhibits synaptic vesicle exocytosis through reduced Ca^{2+} influx rather than Ca^{2+}-exocytosis coupling (Baumgart et al., 2015). In contrast, our results suggest that propofol- and etomidate-mediated presynaptic effects might be directly coupled to the exocytosis machinery. Whether this is a difference between intravenous and volatile anesthetics is unclear. Nevertheless, a set of distinct presynaptic mechanisms linked to exocytosis might explain why recovery from general anesthesia appears to involve a different process than anesthesia induction (Friedman et al., 2010; van Swinderen and Kottler, 2014); re-establishing functional connectivity after neurotransmission has returned to normal levels across the brain would likely involve a different process than falling asleep or waking up. It will be interesting in future research to use transgenic syntaxin1A animals (Zalucki et al., 2015) to link the local effects we have found at the presynapse with consequent changes in global readouts, such as whole-brain connectivity and coherence (Cohen et al., 2016).

EXPERIMENTAL PROCEDURES

For a detailed description of the experimental procedures, see Supplemental Experimental Procedures.

Construction of Genetic Constructs

Rat syntaxin1A-mEos2 and *Drosophila* syntaxin1A-mEos2 were constructed as previously described (Bademosi et al., 2017; Kasula et al., 2016). Syntaxin1A deletions (Δ183–265 and Δ204–250) were generated (from rat syntaxin1A) (Table S1) and truncated syntaxin1A ($Sx1A^{227}$) from full-length *Drosophila* syntaxin1A.

Cell Culture and DNA Transfection

PC12 cells were cultured in DMEM as previously described (Kasula et al., 2016). Plasmid transfection was carried out with Lipofectamine reagent (Invitrogen).

Drosophila melanogaster Stocks

Syntaxin1A-mEos2 flies were generated using standard procedures (Bademosi et al., 2017) and housed at room temperature (25°C).

sptPALM

For sptPALM of transfected PC12 cells, imaging was carried out on the Roper Scientific TIRF microscope. In *Drosophila* larvae, sptPALM was carried out with oblique illumination using a TIRF-enabled ELYRA PS.1 microscope (Zeiss) as previously described (Bademosi et al., 2017). Data analysis was carried out using PALM-Tracer, a plugin in Metamorph software (Molecular Devices).

Single-Molecule Localization Microscopy and Cluster Analysis

PC12 cells or *Drosophila* third-instar larvae were fixed with 4% paraformaldehyde. Single-molecule localization was carried out on an ELYRA PS1 microscope. The datasets were reconstructed with a pixel size of 10 nm, and regions of interest (ROIs) were selected from reconstructed 2D histograms. A custom-written program (Harper et al., 2016) in MATLAB (The MathWorks, 2014) quantified the clustering of the proteins using an autocorrelation function. For each PC12 cell or *Drosophila* larva NMJ chain, 3 different ROIs were drawn, and the extracted data were averaged to represent one dataset per cell.

General Anesthetic Concentration

The concentrations of drugs used in this study were determined by spectrophotometric absorbance readings.

NPY-hPLAP Release Assay

PC12 cells were transfected with NPY fused to the catalytic domain of human placental alkaline phosphatase (NPY-hPLAP) for 48 hr. NPY-hPLAP released from cells was measured using the chemiluminescent reporter gene assay system (Phospha-Light; Applied Biosystems) according to the manufacturer's instructions.

Focal Macropatch Recordings from Single Synaptic Boutons

Postsynaptic currents were measured from individual type 1b boutons using beveled glass electrodes (Karunanithi et al., 1999, 2002).

SUPPLEMENTAL INFORMATION

Supplemental Information includes Supplemental Experimental Procedures, seven figures, one table, and two movies and can be found with this article online at https://doi.org/10.1016/j.celrep.2017.12.054.

ACKNOWLEDGMENTS

We thank members of the van Swinderen, Meunier, and Anggono labs for critical feedback on the experiments and manuscript. This work was supported by the National Health and Medical Research Council (NHMRC) (project grant APP1103923 to B.v.S. and V.A.) and the Australian Research Council (ARC) (LIEF Grant LE0882864 to F.A.M.; LIEF grant LE130100078 to F.A.M. and S.K.; DP170100125 to F.A.M.; DP1093968 to B.v.S.).

AUTHOR CONTRIBUTIONS

A.T.B., J.S., S.K., O.H.Z., R.S.G., and S.L. performed experiments and analyzed data. E.L., P.V., V.A., and F.A.M. provided reagents and infrastructure for the experiments. A.T.B., V.A., F.A.M., and B.v.S. designed the study. A.T.B. and B.v.S. wrote the paper.

DECLARATION OF INTERESTS

The authors declare no competing interests.

Received: July 12, 2017
Revised: October 27, 2017
Accepted: December 15, 2017
Published: January 9, 2018

REFERENCES

Bademosi, A.T., Lauwers, E., Padmanabhan, P., Odierna, L., Chai, Y.J., Papadopulos, A., Goodhill, G.J., Verstreken, P., van Swinderen, B., and Meunier, F.A. (2017). In vivo single-molecule imaging of syntaxin1A reveals polyphosphoinositide- and activity-dependent trapping in presynaptic nanoclusters. Nat. Commun. *8*, 13660.

Bahri, M.A., Seret, A., Hans, P., Piette, J., Deby-Dupont, G., and Hoebeke, M. (2007). Does propofol alter membrane fluidity at clinically relevant concentrations? An ESR spin label study. Biophys. Chem. *129*, 82–91.

Bajohrs, M., Rickman, C., Binz, T., and Davletov, B. (2004). A molecular basis underlying differences in the toxicity of botulinum serotypes A and E. EMBO Rep. *5*, 1090–1095.

Bali, M., and Akabas, M.H. (2004). Defining the propofol binding site location on the GABAA receptor. Mol. Pharmacol. *65*, 68–76.

Bar-On, D., Wolter, S., van de Linde, S., Heilemann, M., Nudelman, G., Nachliel, E., Gutman, M., Sauer, M., and Ashery, U. (2012). Super-resolution imaging reveals the internal architecture of nano-sized syntaxin clusters. J. Biol. Chem. *287*, 27158–27167.

Barg, S., Knowles, M.K., Chen, X., Midorikawa, M., and Almers, W. (2010). Syntaxin clusters assemble reversibly at sites of secretory granules in live cells. Proc. Natl. Acad. Sci. USA *107*, 20804–20809.

Baumgart, J.P., Zhou, Z.Y., Hara, M., Cook, D.C., Hoppa, M.B., Ryan, T.A., and Hemmings, H.C., Jr. (2015). Isoflurane inhibits synaptic vesicle exocytosis through reduced Ca2+ influx, not Ca2+-exocytosis coupling. Proc. Natl. Acad. Sci. USA *112*, 11959–11964.

Boly, M., Moran, R., Murphy, M., Boveroux, P., Bruno, M.A., Noirhomme, Q., Ledoux, D., Bonhomme, V., Brichant, J.F., Tononi, G., et al. (2012). Connectivity changes underlying spectral EEG changes during propofol-induced loss of consciousness. J. Neurosci. *32*, 7082–7090.

Brown, E.N., Purdon, P.L., and Van Dort, C.J. (2011). General anesthesia and altered states of arousal: a systems neuroscience analysis. Annu. Rev. Neurosci. *34*, 601–628.

Chennu, S., O'Connor, S., Adapa, R., Menon, D.K., and Bekinschtein, T.A. (2016). Brain connectivity dissociates responsiveness from drug exposure during propofol-induced transitions of consciousness. PLoS Comput. Biol. *12*, e1004669.

Cohen, D., Zalucki, O.H., van Swinderen, B., and Tsuchiya, N. (2016). Local versus global effects of isoflurane anesthesia on visual processing in the fly brain. eNeuro *3*, ENEURO.0116-16.2016.

Ferro-Novick, S., and Jahn, R. (1994). Vesicle fusion from yeast to man. Nature *370*, 191–193.

Franks, N.P. (2006). Molecular targets underlying general anaesthesia. Br. J. Pharmacol. *147* (*Suppl 1*), S72–S81.

Franks, N.P. (2008). General anaesthesia: from molecular targets to neuronal pathways of sleep and arousal. Nat. Rev. Neurosci. *9*, 370–386.

Franks, N.P., and Lieb, W.R. (1994). Molecular and cellular mechanisms of general anaesthesia. Nature *367*, 607–614.

Friedman, E.B., Sun, Y., Moore, J.T., Hung, H.T., Meng, Q.C., Perera, P., Joiner, W.J., Thomas, S.A., Eckenhoff, R.G., Sehgal, A., and Kelz, M.B. (2010). A conserved behavioral state barrier impedes transitions between anesthetic-induced unconsciousness and wakefulness: evidence for neural inertia. PLoS ONE *5*, e11903.

Gandasi, N.R., and Barg, S. (2014). Contact-induced clustering of syntaxin and munc18 docks secretory granules at the exocytosis site. Nat. Commun. *5*, 3914.

Giese, J.L., and Stanley, T.H. (1983). Etomidate: a new intravenous anesthetic induction agent. Pharmacotherapy *3*, 251–258.

Harper, C.B., Papadopulos, A., Martin, S., Matthews, D.R., Morgan, G.P., Nguyen, T.H., Wang, T., Nair, D., Choquet, D., and Meunier, F.A. (2016). Botulinum neurotoxin type-A enters a non-recycling pool of synaptic vesicles. Sci. Rep. *6*, 19654.

Hayashi, T., McMahon, H., Yamasaki, S., Binz, T., Hata, Y., Südhof, T.C., and Niemann, H. (1994). Synaptic vesicle membrane fusion complex: action of clostridial neurotoxins on assembly. EMBO J. *13*, 5051–5061.

Heldman, E., Levine, M., Raveh, L., and Pollard, H.B. (1989). Barium ions enter chromaffin cells via voltage-dependent calcium channels and induce secretion by a mechanism independent of calcium. J. Biol. Chem. *264*, 7914–7920.

Herring, B.E., Xie, Z., Marks, J., and Fox, A.P. (2009). Isoflurane inhibits the neurotransmitter release machinery. J. Neurophysiol. *102*, 1265–1273.

Herring, B.E., McMillan, K., Pike, C.M., Marks, J., Fox, A.P., and Xie, Z. (2011). Etomidate and propofol inhibit the neurotransmitter release machinery at different sites. J. Physiol. *589*, 1103–1115.

Hudetz, A.G. (2012). General anesthesia and human brain connectivity. Brain Connect. *2*, 291–302.

Karunanithi, S., Barclay, J.W., Robertson, R.M., Brown, I.R., and Atwood, H.L. (1999). Neuroprotection at Drosophila synapses conferred by prior heat shock. J. Neurosci. *19*, 4360–4369.

Karunanithi, S., Marin, L., Wong, K., and Atwood, H.L. (2002). Quantal size and variation determined by vesicle size in normal and mutant Drosophila glutamatergic synapses. J. Neurosci. *22*, 10267–10276.

Kasula, R., Chai, Y.J., Bademosi, A.T., Harper, C.B., Gormal, R.S., Morrow, I.C., Hosy, E., Collins, B.M., Choquet, D., Papadopulos, A., and Meunier, F.A. (2016). The Munc18-1 domain 3a hinge-loop controls syntaxin-1A nanodomain assembly and engagement with the SNARE complex during secretory vesicle priming. J. Cell Biol. *214*, 847–858.

Krasowski, M.D., Jenkins, A., Flood, P., Kung, A.Y., Hopfinger, A.J., and Harrison, N.L. (2001). General anesthetic potencies of a series of propofol analogs correlate with potency for potentiation of gamma-aminobutyric acid (GABA) current at the GABA(A) receptor but not with lipid solubility. J. Pharmacol. Exp. Ther. *297*, 338–351.

Lewis, L.D., Weiner, V.S., Mukamel, E.A., Donoghue, J.A., Eskandar, E.N., Madsen, J.R., Anderson, W.S., Hochberg, L.R., Cash, S.S., Brown, E.N., and Purdon, P.L. (2012). Rapid fragmentation of neuronal networks at the onset of propofol-induced unconsciousness. Proc. Natl. Acad. Sci. USA *109*, E3377–E3386.

McKinney, S.A., Murphy, C.S., Hazelwood, K.L., Davidson, M.W., and Looger, L.L. (2009). A bright and photostable photoconvertible fluorescent protein. Nat. Methods *6*, 131–133.

Merklinger, E., Schloetel, J.G., Weber, P., Batoulis, H., Holz, S., Karnowski, N., Finke, J., and Lang, T. (2017). The packing density of a supramolecular membrane protein cluster is controlled by cytoplasmic interactions. eLife *6*, e20705.

Metz, L.B., Dasgupta, N., Liu, C., Hunt, S.J., and Crowder, C.M. (2007). An evolutionarily conserved presynaptic protein is required for isoflurane sensitivity in Caenorhabditis elegans. Anesthesiology *107*, 971–982.

Miesenböck, G., De Angelis, D.A., and Rothman, J.E. (1998). Visualizing secretion and synaptic transmission with pH-sensitive green fluorescent proteins. Nature *394*, 192–195.

Nagele, P., Mendel, J.B., Placzek, W.J., Scott, B.A., D'Avignon, D.A., and Crowder, C.M. (2005). Volatile anesthetics bind rat synaptic snare proteins. Anesthesiology *103*, 768–778.

Pertsinidis, A., Mukherjee, K., Sharma, M., Pang, Z.P., Park, S.R., Zhang, Y., Brunger, A.T., Südhof, T.C., and Chu, S. (2013). Ultrahigh-resolution imaging reveals formation of neuronal SNARE/Munc18 complexes in situ. Proc. Natl. Acad. Sci. USA *110*, E2812–E2820.

Ribrault, C., Reingruber, J., Petković, M., Galli, T., Ziv, N.E., Holcman, D., and Triller, A. (2011). Syntaxin1A lateral diffusion reveals transient and local SNARE interactions. J. Neurosci. *31*, 17590–17602.

Rickman, C., Meunier, F.A., Binz, T., and Davletov, B. (2004). High affinity interaction of syntaxin and SNAP-25 on the plasma membrane is abolished by botulinum toxin E. J. Biol. Chem. *279*, 644–651.

Rudolph, U., and Antkowiak, B. (2004). Molecular and neuronal substrates for general anaesthetics. Nat. Rev. Neurosci. *5*, 709–720.

Sall, J.W., Stratmann, G., Leong, J., Woodward, E., and Bickler, P.E. (2012). Propofol at clinically relevant concentrations increases neuronal differentiation but is not toxic to hippocampal neural precursor cells in vitro. Anesthesiology *117*, 1080–1090.

Sengupta, P., Jovanovic-Talisman, T., and Lippincott-Schwartz, J. (2013). Quantifying spatial organization in point-localization superresolution images using pair correlation analysis. Nat. Protoc. *8*, 345–354.

Sieber, J.J., Willig, K.I., Kutzner, C., Gerding-Reimers, C., Harke, B., Donnert, G., Rammner, B., Eggeling, C., Hell, S.W., Grubmüller, H., and Lang, T. (2007). Anatomy and dynamics of a supramolecular membrane protein cluster. Science *317*, 1072–1076.

Sudhof, T.C. (2004). The synaptic vesicle cycle. Annu. Rev. Neurosci. *27*, 509–547.

Südhof, T.C., and Rizo, J. (2011). Synaptic vesicle exocytosis. Cold Spring Harb. Perspect. Biol. *3*, a005645.

Südhof, T.C., and Rothman, J.E. (2009). Membrane fusion: grappling with SNARE and SM proteins. Science *323*, 474–477.

Ton, H.T., Phan, T.X., Abramyan, A.M., Shi, L., and Ahern, G.P. (2017). Identification of a putative binding site critical for general anesthetic activation of TRPA1. Proc. Natl. Acad. Sci. USA *114*, 3762–3767.

Tsuchiya, H. (2001). Structure-specific membrane-fluidizing effect of propofol. Clin. Exp. Pharmacol. Physiol. *28*, 292–299.

Tsuchiya, H., Ueno, T., Tanaka, T., Matsuura, N., and Mizogami, M. (2010). Comparative study on determination of antioxidant and membrane activities of propofol and its related compounds. Eur. J. Pharm. Sci. *39*, 97–102.

van Swinderen, B., and Kottler, B. (2014). Explaining general anesthesia: a two-step hypothesis linking sleep circuits and the synaptic release machinery. BioEssays *36*, 372–381.

Veatch, S.L., Machta, B.B., Shelby, S.A., Chiang, E.N., Holowka, D.A., and Baird, B.A. (2012). Correlation functions quantify super-resolution images and estimate apparent clustering due to over-counting. PLoS ONE *7*, e31457.

Wang, S., Choi, U.B., Gong, J., Yang, X., Li, Y., Wang, A.L., Yang, X., Brunger, A.T., and Ma, C. (2017). Conformational change of syntaxin linker region induced by Munc13s initiates SNARE complex formation in synaptic exocytosis. EMBO J. *36*, 816–829.

Weiser, B.P., Kelz, M.B., and Eckenhoff, R.G. (2013). In vivo activation of azipropofol prolongs anesthesia and reveals synaptic targets. J. Biol. Chem. *288*, 1279–1285.

Weninger, K., Bowen, M.E., Chu, S., and Brunger, A.T. (2003). Single-molecule studies of SNARE complex assembly reveal parallel and antiparallel configurations. Proc. Natl. Acad. Sci. USA *100*, 14800–14805.

Weninger, K., Bowen, M.E., Choi, U.B., Chu, S., and Brunger, A.T. (2008). Accessory proteins stabilize the acceptor complex for synaptobrevin, the 1:1 syntaxin/SNAP-25 complex. Structure *16*, 308–320.

Wu, M.N., Fergestad, T., Lloyd, T.E., He, Y., Broadie, K., and Bellen, H.J. (1999). Syntaxin 1A interacts with multiple exocytic proteins to regulate neurotransmitter release in vivo. Neuron *23*, 593–605.

Xiao, W., Poirier, M.A., Bennett, M.K., and Shin, Y.K. (2001). The neuronal t-SNARE complex is a parallel four-helix bundle. Nat. Struct. Biol. *8*, 308–311.

Xie, Z., McMillan, K., Pike, C.M., Cahill, A.L., Herring, B.E., Wang, Q., and Fox, A.P. (2013). Interaction of anesthetics with neurotransmitter release machinery proteins. J. Neurophysiol. *109*, 758–767.

Yang, X., Wang, S., Sheng, Y., Zhang, M., Zou, W., Wu, L., Kang, L., Rizo, J., Zhang, R., Xu, T., and Ma, C. (2015). Syntaxin opening by the MUN domain underlies the function of Munc13 in synaptic-vesicle priming. Nat. Struct. Mol. Biol. *22*, 547–554.

Yip, G.M., Chen, Z.W., Edge, C.J., Smith, E.H., Dickinson, R., Hohenester, E., Townsend, R.R., Fuchs, K., Sieghart, W., Evers, A.S., and Franks, N.P. (2013). A propofol binding site on mammalian GABAA receptors identified by photolabeling. Nat. Chem. Biol. *9*, 715–720.

Zalucki, O.H., Menon, H., Kottler, B., Faville, R., Day, R., Bademosi, A.T., Lavidis, N., Karunanithi, S., and van Swinderen, B. (2015). Syntaxin1A-mediated resistance and hypersensitivity to isoflurane in Drosophila melanogaster. Anesthesiology *122*, 1060–1074.

Zilly, F.E., Halemani, N.D., Walrafen, D., Spitta, L., Schreiber, A., Jahn, R., and Lang, T. (2011). Ca2+ induces clustering of membrane proteins in the plasma membrane via electrostatic interactions. EMBO J. *30*, 1209–1220.